

# Advanced DIC Post-processing Technique to Analyze Biaxial Bulge Test

Amir Asgharzadeh and Laura Zoller, EWI

Material flow stress is an important input for numerical modeling of sheet metal forming processes. The uniaxial tensile test (UTT) is widely employed to determine the flow curve of sheet metals. However, the range of strain obtained from UTT is limited, so extending plastic flow behavior is required for accurate simulations of most forming processes. Different material hardening models such as Holloman, Swift, Ludwick, and Voce have been developed to extrapolate the material's flow stress obtained from the UTT.<sup>1</sup> The estimation of flow curve beyond the limit of uniform strain through various hardening models could impose uncertainty to the obtained stress data.<sup>2</sup> Therefore, a mechanical test that is able to obtain material flow stress at the larger plastic strain is preferred.<sup>3</sup>

The hydraulic bulge test (HBT) is used to experimentally obtain the material's flow curve at extended uniform strains as an alternative method.<sup>4</sup> The membrane theory developed by Hill for the sheet metals deformed by internal pressure is adopted to obtain the flow stress in the bulged specimen.<sup>5</sup> According to this theory, the instantaneous curvature and thickness of the sheet material throughout the bulge test are required to calculate the biaxial stress components at the pole of the bulged sample. In the traditional HBT, the measurement of the dome curvature and blank thickness is conducted

manually, which has been extremely challenging. Using digital image correlation (DIC), advanced data processing approaches have been developed to determine curvature and thickness more accurately throughout the HBT. With novel methods developed for analysis of HBT DIC data, the accuracy of the measurement of biaxial curvatures, biaxial strain, and anisotropic material behavior has improved.<sup>6</sup> Although progress has been achieved in obtaining test parameters to calculate the material's flow stress through HBT, how to properly process DIC data to precisely obtain stress-strain data at larger strains is still an open question.

## Experimental Hydraulic Bulge Test

In this study, 980 GEN3 steel with 1.2-mm thickness was used. To assess material properties, both UTT and HBT were performed. The uniaxial tensile test was performed using INSTRON tensile testing machine under 3 mm/min. RAM speed. The HBT was performed using the Erichsen sheet metal testing machine. A blank holding force of 400 kN was applied to clamp the sample during the test while the hydraulic pressure was applied to the blank with a pressurized oil. The outer surface of the blank was

used to measure the displacement field throughout the bulge test using DIC equipment. The DIC measurement was performed according to the *Good Practices Guide for Digital Image Correlation*.<sup>7</sup> After the HBT, the synchronized pressure-displacement data was put into to the analytical model based on membrane theory to generate the flow stress-strain data under biaxial deformation mode.

## Analytical Model to Determine Biaxial Stress-strain Curve

To determine the biaxial stress-strain curve using HBT, an analytical model based on the membrane theory was used.<sup>5</sup> According to the membrane theory, the equilibrium equation for an axially symmetric element under the uniform pressure is the following:

$$\frac{\sigma_1}{\rho_1} + \frac{\sigma_2}{\rho_2} = \frac{p}{t} \quad \text{Equation 1}$$

where,  $\sigma_1$  and  $\sigma_2$  are the principal in-plane stress components,  $\rho_1$  and  $\rho_2$  are curvature radii of the bulge dome in two principal directions,  $p$  is the internal pressure, and  $t$  is the thickness of the specimen. Assuming isothermal material behavior and spherical bulge dome geometry, Eq. 1 is re-written as follows:

$$\rho_1 = \rho_2 = \rho \quad \& \quad \sigma_1 = \sigma_2 = \sigma_b \quad \text{Equation 2}$$

$$\sigma_b = \frac{\rho \cdot p}{2t} \quad \text{Equation 3}$$

where  $\sigma_b$  is the equivalent biaxial stress.<sup>9</sup> The principal in-plane strain components obtained from DIC data is used to calculate  $t$ . Assuming plastic incompressibility

and neglecting elastic strains, the thickness of specimen is calculated as follows:

$$t = t_0 \exp(-(\varepsilon_1 + \varepsilon_2)) \quad \text{Equation 4}$$

where  $t_0$  is initial thickness of the blank, and  $\varepsilon_1$  and  $\varepsilon_2$  are principal in-plane, true-strain components obtained from DIC data.<sup>10</sup> In addition, the isotropic von Mises material model is used to calculate the equivalent biaxial stress and strain within the bulged specimen.<sup>10</sup>

To obtain the biaxial stress-strain curve through equations 1 to 4, three variables from HBT were required: the internal pressure ( $p$ ) which was recorded during HBT, the dome curvature ( $\rho$ ) that was obtained through the least-squares-fitting method on the X-Y-Z coordinates near the apex of the dome, and the thickness ( $t$ ) that was calculated from the in-plane strain components near the apex of the dome. The coordinate and strain data were obtained from DIC data measured throughout HBT.

## Results

UTT and HBT were performed to obtain the flow stress of the sheet materials, in which the load-displacement and pressure-displacement data, respectively, were used to generate the corresponding stress-strain curves. The load and pressure data were collected using a data logger installed on the mechanical testing machine, while displacement data was acquired through DIC measurement. The DIC measurement of true major strain as well as the stress-strain curve obtained from UTT performed on 980GEN3 steel are shown in Figure 1. To obtain the strain data from DIC measurement, a virtual extensometer over the entire 60-mm gauge length was created (Figure 1a) and the corresponding displacement data was used to calculate the true strain. The data shown

in Figure 1b verifies the repeatability and validity of the performed UTT on 980 GEN3 steel.

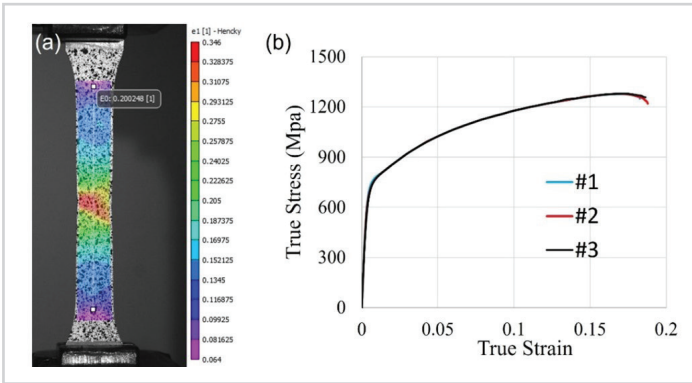


Figure 1. a) The DIC measurement of true major strain and b) the UTT stress-strain curve of 980GEN3

The HBT was used to determine the material’s flow curve at larger plastic. To obtain membrane theory inputs for calculation of the biaxial flow stress, as demonstrated in equations 1 to 4, DIC measurement was performed to obtain the instantaneous curvature and thickness of the sheet material throughout the bulge test. The curvature of the bulged dome was obtained through the least-squares-fitting method on the X-Y-Z coordinates along the arc crossing the pole of the bulged sample, while the thickness was calculated through obtaining the in-plane principal strain components from the DIC data.

A post analysis performed on DIC data obtained through HBT showed that arc length crossing the pole of the bulged sample significantly impacted the calculated curvature and ultimately the calculated biaxial stress. Figure 2 shows the sensitivity of the dome radii to the arc length. In Figure 2b, the dome radius at a lower dome height shows a large variation. The variation was reduced as the dome height was increased. However, it was observed that the increase in the arc length did not lead to convergence in the calculated dome radius throughout the bulge test. The variation in the calculated dome radius results in the variation of the obtained biaxial flow curve.

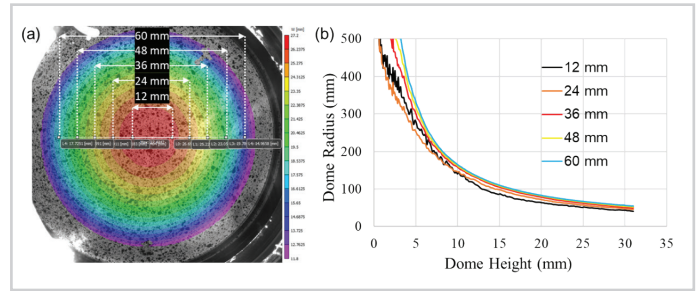


Figure 2. Effect of arc length on the dome radius: a) the DIC measurement of true major strain and b) the dome radius versus dome height at different arc lengths

To generate the biaxial stress-strain curve from the DIC data, the in-plane major and minor strains were extracted to calculate instantaneous sheet thickness and equivalent strain throughout the bulge test. To do this, the major and minor strains along the arcs were exported and averaged over the entire arc length. To understand the deformation behavior within the bulged specimen, the sensitivity of strain path and the calculated sheet thickness to the arc length were investigated. Figure 3a shows the major-minor strain path for each created arc throughout HBT. The strain path over the 12-mm and 24-mm arcs was similar to the strain path of the point on the apex of the dome, while it deviated from the equi-biaxial condition as the arc length got larger than 24 mm. Figure 3b shows the variation of the sheet thickness over the length of the arc in the last DIC image before the fracture. As seen, a more uniform thickness distribution could be obtained by taking the shorter arc length, while the longer arcs would lead to severe thickness inhomogeneity over the arc length.

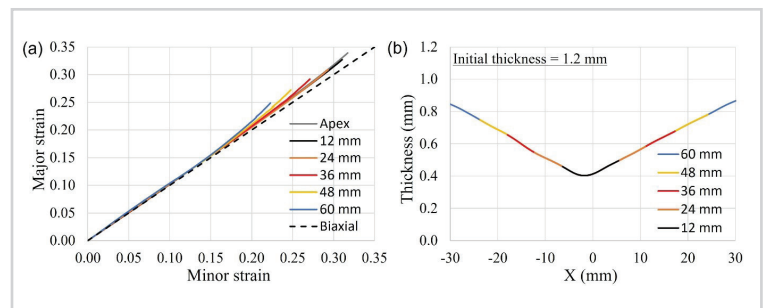


Figure 3. Sensitivity of a) the strain path and b) the blank thickness to the arc length according to Figure 5a

Similar to the dome radius, the variation in the sheet thickness directly impacted the biaxial flow curve as it was directly used as an input to the membrane theory for the calculation of the biaxial stress.

Figure 4a shows the biaxial stress-strain curve for 980 GEN3 corresponding to the different arcs created in Figure 2a. To obtain the flow curve corresponding to each arc length, the instantaneous dome radius and sheet thickness (Figures 2b and 3b, respectively) were used to calculate the biaxial flow stress. Furthermore, the equivalent strain was calculated by averaging out the major and minor strain components along the created arcs. The results show that the flow stress was quite sensitive to the arc length, so that the higher strain hardening rate and smaller total equivalent strain were achieved by considering longer arc length. In addition, the necking point corresponding to each curve was plotted to identify the uniform elongation limit during HBT. To obtain the necking point, the major and minor strain data were exported from the pole of the bulged tube and the linear best fit (LBF) method was utilized to detect the necking strains (For details of the LBF technique, see Recheck et al.<sup>11</sup>). The uniform and total equivalent true strains obtained from the HBT DIC data is plotted in Figure 4b which shows that the uniform and total equivalent strains slightly increased by reducing the arc length. The maximum uniform and total equivalent strain were obtained on the apex of the dome, in which the most localized strain data was exported from DIC data.

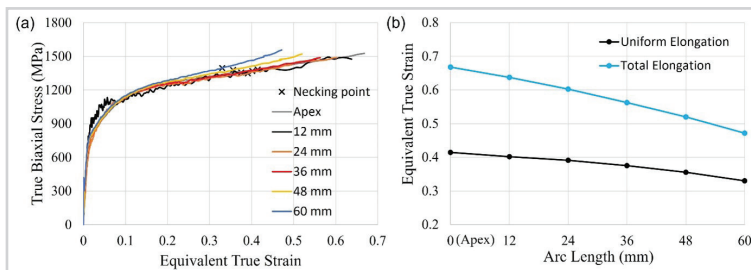


Figure 4. Effect of arc length on a) the biaxial flow curve and b) the corresponding uniform and total equivalent strains obtained from HBT.

The variation of the biaxial stress-strain curve depicted in Figure 4a raised a question about the flow curve corresponding to which arc length actually represented the material's biaxial flow stress. To address this issue, the plastic work equivalency principal was adopted to compare the biaxial stress-strain curve with the UTT flow curve within the uniform strain region. In other words, the plastic work obtained from biaxial flow curves (Figure 4-a) was compared to the plastic work obtained from the uniaxial flow curve (Figure 1-b) within the uniform strain region. Then, the biaxial stress-strain curve with the best-fit plastic work equivalency to UTT flow stress was chosen as the actual biaxial flow stress. The plastic work ( $w^P$ ) was calculated as follows:<sup>12</sup>

$$dw^P = \bar{\sigma} d\bar{\epsilon}^P \quad \text{Equation 5}$$

where  $\bar{\sigma}$  and  $\bar{\epsilon}$  denote the equivalent stress and strain, respectively. The comparison of the plastic work versus equivalent true strain obtained from biaxial and uniaxial flow curves within the uniform strain region is illustrated in Figure 5a. The best match in the plastic work obtained from HBT and UTT is shown in Figure 5b, which confirms that the HBT flow curve obtained through 48-mm arc length represent the accurate material's flow stress.

Based on the best-fit plastic work equivalency obtained in Figure 5b, the representative biaxial flow stress of 980GEN3 was observed (see Figure 6). Since the flow stress up to the uniform strain was useful in FE simulation, the necking point corresponding to the final biaxial flow curve has also been indicated in Figure 6. The maximum uniform equivalent strain obtained through HBT was 0.36, which is twice as large as the maximum uniform strain of 0.17 obtained through UTT (see Figure 1). However, it is worthwhile to note that the biaxial flow data obtained beyond this strain limit may include some degree of uncertainty due to the non-uniform deformation behavior.

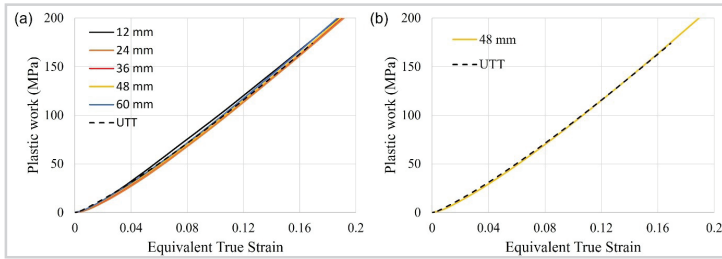


Figure 5. a) The comparison of the plastic work versus equivalent true strain obtained from biaxial and uniaxial flow curves, and b) the best match in the plastic work obtained within the uniform strain region.

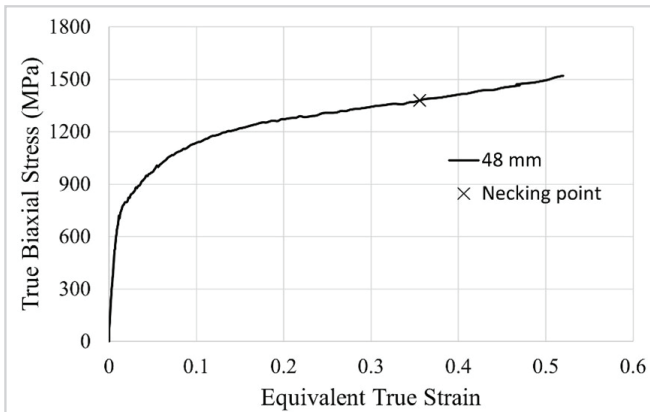


Figure 6. The representative biaxial flow stress of 980GEN3.

## Conclusions

The hydraulic bulge test was performed on 980 GEN3 steel to obtain the flow stress at extended uniform equivalent strain compared to the uniaxial deformation condition. An elaborative study based on DIC data analysis was performed to define the sensitivity of the calculated biaxial flow curve to the process variables obtained through DIC measurements. The results showed that:

- The biaxial flow stress in the plastic deformation region was sensitive to the arc length created in DIC data of

bulge specimen to export strain data. The shorter arc on the bulged specimen would lead to higher uniform strain limit, lower strain hardening rate, and uniform thickness distribution, with the cost of imposing uncertainty in the calculation of curvature.

- By adopting the plastic work equivalency principal, the optimal arc length for calculation of the biaxial flow curve was obtained, in which the maximum uniform equivalent strain is more than twice the maximum uniform strain obtained through uniaxial flow curve.

For more information about these techniques, contact Laura Zoller at [lzoller@ewi.org](mailto:lzoller@ewi.org).

**Note:** Any reference to specific equipment and/or materials is for informational purposes only. Any reference made to a specific product does not constitute or imply an endorsement by EWI of the product or its producer or provider.

### References

- 1 Asgharzadeh, A., Tiji S. A. N., Esmailpour, R., Park, T., and Pourboghrat, F. (2020). Determination of hardness-strength and -flow behavior relationships in bulged aluminum alloys and verification by FE analysis on Rockwell hardness test. *J. Adv. Manuf. Technol.*, (106), 315-331.
- 2 Zhang, S., Leotoing, L., Guines, D., Thuillier, S., and Zang, S. L. (2014). Calibration of anisotropic yield criterion with conventional tests or biaxial test. *Int. J. Mech. Sci.* (85), 142-151.
- 3 Min, J., Stoughton, T. B., Carsley, J. E., Carlson, B. E., Lin, J., Gao, X. (2017). Accurate characterization of biaxial stress-strain response of sheet metal from bulge testing. *Int. J. Plast.* (94), 192-213.
- 4 Atkinson, M. (1997). Accurate determination of biaxial stress-strain relationships from hydraulic bulging tests of sheet metals. *Int. J. Mech. Sci.* (39), 761-769.
- 5 Hill, R. (1950). A theory of the plastic bulging of a metal diaphragm by lateral pressure. *The London, Edinburgh, and Dublin Philosophical Magazine and Journal of Science* (41), 1133-1142.
- 6 Rossi, M., Lattanzi, A., Barlat, F., and Kim, J. H. (2022). Inverse identification of large strain plasticity using the hydraulic bulge-test and full-field measurements. *Int. J. Solids Struct.* (242) 111532
- 7 Jones, E. M. C., and Iadicola, M. A. (2018) A good practices guide for digital image correlation. *International Digital Image Correlation Society*

- 8 Billur, E. (2020) Digital image correlation: How it changed the bulge test. *Metal Forming Magazine*
- 9 Lăzărescu, L., Comşa, D. S., Nicodim, I., Ciobanu, I., and Banabic, D. (2012) Characterization of plastic behaviour of sheet metals by hydraulic bulge test. *Trans. Nonferrous Met. Soc.* (22), 275-279.
- 10 Asgharzadeh, A., Tiji S. A. N. , Park, T., Kim, J. H., and Pourboghra, F. (2020) Cellular automata modeling of the kinetics of static recrystallization during the post-hydroforming annealing of steel tube. *J. Mater. Sci.* (55), 7938-7957.
- 11 Rencheck, M., Zelenak, P., Shang, J. and Kim, H. (2017). Evaluation of DIC based forming limit curve methods at various temperatures of aluminum alloys for automotive applications. *SAE Technical Paper* (2017-01-0309).
- 12 Tiji S. A. N. , Park, T., Asgharzadeh, A., Kim, H., Athale, M., Kim, J. H., and Pourboghra, F. (2020) Characterization of yield stress surface and strain-rate potential for tubular materials using multiaxial tube expansion test method. *Int. J. Plast.* (133), 102838

---

**Amir Asgharzadeh** is Project Engineer for the forming team at EWI. His area of expertise resides at the interface of solid mechanics, metal forming processes, and materials modeling. He has in-depth knowledge of computational sciences and experimental mechanics with focus on studying the formability of conventional and advanced metallic materials.

---

**Laura Zoller** is Engineering Manager for EWI's forming, laser, structural integrity, NDE, and materials engineering teams. She has professional expertise in processing, measuring, and analyzing materials used for sheet metal forming. She operates EWI's stamping presses and equipment, leads quality inspection testing on final part geometries and tooling, and conducts material formability tests and research on non-ferrous and steel sheet metal.